Available online at www.sciencedirect.com

ScienceDirect

Procedia Engineering 183 (2017) 369 – 374

Procedia Engineering

www.elsevier.com/locate/procedia

17th International Conference on Sheet Metal, SHEMET17

Reverse analysis of scan strategies for controlled 3D laser forming of sheet metal

H. Gao[a]*, G. Sheikholeslami[b], G. Dearden[c], S. P. Edwardson[d]*

Laser Engineering Group, School of Engineering,University of Liverpool,Brownlow Street, Liverpool L69 3GQ,UK

Abstract

Laser forming is an advanced manufacturing technique for the shaping and adjustment of metallic and non-metallic components by controlled laser induced thermal stress. Important advantages of laser forming include the absence of external mechanical tooling, flexibility and potential for automatic control. A large number of relevant two-dimensional laser forming studies have been completed to date. However, for the production of complex 3D shapes, such as ship hull components, airplane fuselages and automotive bodies, two-dimensional laser forming is limited. Therefore, in order to advance process for realistic applications, the investigation of the 3D scanning strategies becomes essential. This includes both in plane shortening and out-of-plane bending. In order to determining the scanning patterns and process parameters for forming any arbitrary 3D shape, numerical simulation is a strong tool to analyse the required stress and strain distribution and related processing parameters. In the presented investigation, the object is to develop optimal irradiation patterns and parameters to form a S275 steel square thin plate to a given generic ship hull shape through finite element simulation and experiment verification. A novel approach was used for the development of scan strategies for controlled 3D laser forming of sheet metal components based on a reverse analysis. A patched modular virtual press tool was employed in a commercial FE package COMSOL Multiphysics to extract the required strain-displacement map to achieve a given shape from a starting condition. The laser processing conditions have then been extracted from the magnitude of strain and displacement of each patch. A closed loop control iterative approach has then been used to ensure part accuracy during experimental verification.

© 2017 The Authors. Published by Elsevier Ltd. This is an open access article under the CC BY-NC-ND license (http://creativecommons.org/licenses/by-nc-nd/4.0/).
Peer-review under responsibility of the organizing committee of SHEMET17

Keywords: 3D laser forming, FEM simulation, close loop control

* Corresponding author. Tel.:+44-(0)75-362-753-63.
E-mail address: sghgao@liverpool.ac.uk

1877-7058 © 2017 The Authors. Published by Elsevier Ltd. This is an open access article under the CC BY-NC-ND license (http://creativecommons.org/licenses/by-nc-nd/4.0/).
Peer-review under responsibility of the organizing committee of SHEMET17
doi:10.1016/j.proeng.2017.04.054

1. Introduction

In laser forming, the deformation of sheet metal is produced by thermal stresses, which are generated by a controlled defocused laser beam scanned over the surface [1,6]. During laser forming, the non-uniform expansion will occur due to the non-uniform thermal stresses; therefore the plastic deformation will be generated when the thermal stresses exceed the yield point of the material [14].The advantages of laser forming include without any external mechanical tooling, flexibility and automatic control. A large number of relevant two-dimensional laser bending studies have been done to date. However, for the production of complex 3D shapes, such as ship and aerospace surfaces, two-dimensional laser forming is limited [1,3,13]. Therefore, in order to advance process for realistic applications, the investigation of the 3D scanning strategies becomes more necessary, which accompanies both in plane shortening and out-of-plane bending [5,9] as seen in Fig.1. In order to determining the scanning patterns and process parameters for forming any arbitrary 3D shape, numerical simulation is a strong tool to analyse the scan strategies and the processing parameters [6,7].

In the presented investigation, the object is to develop optimal irradiation patterns and parameters to form S275 steel square thin plate with the size of 100×100×1.5mm to a representative ship hull shape. The work consists two parts, finite element simulation and experiment verification. The numerical simulation with two models have been developed by using COMSOL Multiphysics 5.2. One is a virtual press tool mechanical model, and the other is a laser heating thermal mechanical model with a step-wise moving Gaussian distribution of heat flux laser beam.

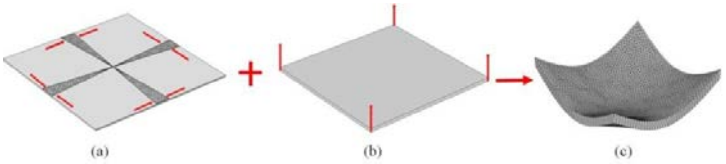

Fig. 1. (a) In-plane shrinkage; (b) Out-of-plane bending; (c) 3D formed shape

2. FEM Simulation

2.1. Determination of the scanning patterns by mechanical model

In the mechanical model, the first step was to decompose the top surface of the initial sheet into a group of sixteen patches with 25 nodal points as shown in Fig.2 (a). The desired shape can be seen in Fig. 2 (b), this is a representative ship hull shape.

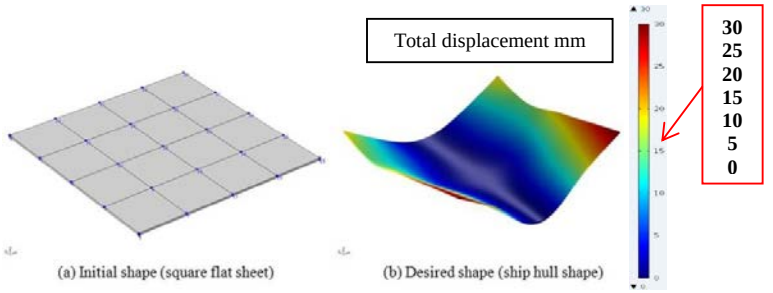

Fig. 2. Definition of the initial shape and desired shape

$$e^I = \frac{1}{h}\int_h^0 e^T \, d_z$$
$$e^B = \frac{1}{h^2}\int_h^0 (e^T - e^I) z d_z \quad (1)$$

From Equation 1 (in-plane e^I and bending strains e^B across the thickness h, e^T is the strains along the thickness), it can be seen that the plastic strain is independent of the material properties. So, the in-plane and bending strain distribution on the heated surface can be obtained by using a virtual press tool to develop an initial shape to the desired shape as shown in Fig.3 (a). The center points on both upper the lower surface were fixed and a positive prescribed displacement on each nodal point was given to develop the target shape. Therefore the scanning paths could be traced perpendicular to the vectors of the averaged in-plane and out of plane strain [10]. Fig.3 (b) plots 4 different proposed heating patterns superposed on the flat sheet. The dense discrete heating line can be regarded as the continuous heating line.

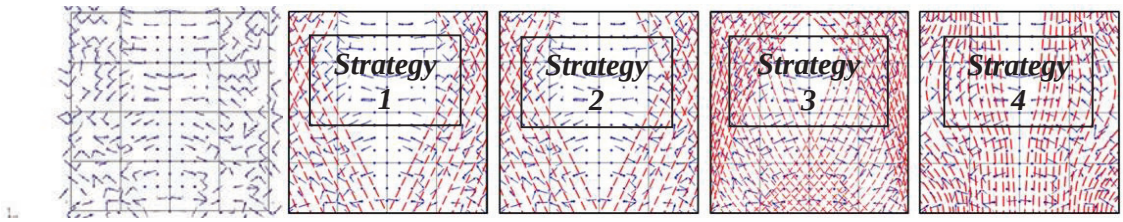

Fig. 3. (a) Vector plot of the summed in-plane strain and bending strain of the given ship hull shape; (b) the determined scanning paths in the red dash line

2.2. Heating Condition Determination by thermo-mechanical model

After determination of the scanning paths, the next step was to determine the required conditions by thermo-mechanical modelling. A critical power density can be obtained for shaping the workpiece without any material damage. According to a large number of experimentally validated simulations, a critical parameter set was obtained, P=500w, d=3mm. V=30mm/sec. The upper limit power density E_0 was found to be 5.5J/mm^2, that is, the material will melt and damage when the power density is over this value.

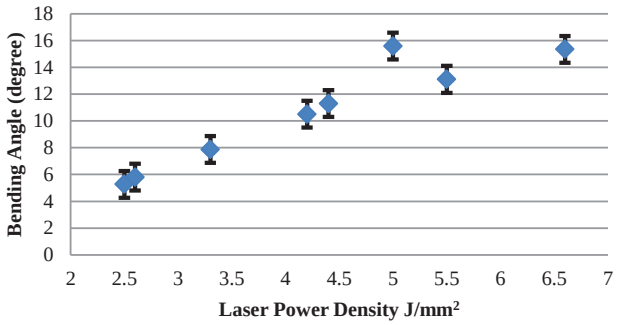

Fig. 4. The effect of laser power density on the bending angle (Pass no. 10 passes, Power range is 400W to 500W, Beam diameter range is 3mm to 5mm. Velocity is from 20 to 40mm/s)

Fig.4 presents the influence of the bending angle with different laser power density experimentally found after 10 passes in a simple 2D bend using a CO_2 laser on graphite coated samples. It can be seen that the bending angle is increasing with the increase of the laser power density and the bending angle converges when the laser power density is over 4.5J/mm^2 due to the coating burn off. Plastic deformation will not be generated when the laser power density is too low due to the thermal stress will not reach the yield stress [12]. It can also be noted that, the controllability is in inverse proportion to the laser power density due to the bending angle produced per pass. The heating parameters on the proposed scanning patterns were decided from a number of simulations, these are

presented in Table 1. These give a power density of 3.3J/mm^2 well below the critical value. This is also in a region where controllability of the process is more likely per pass.

For the thermo-mechanical FE model, the boundary conditions for both solid mechanical and heat transfer analysis are as follows:

A fixed constraint was added to the center of the sample according to the fixtures used in the real experiments. All other boundaries are free and the sample is without any initial residual stress and displacement.

In the heat transfer modelling, the laser beam was modelled to be a Gaussian heat flux distribution on the plate surface, as seen in Eq. (3). The thermal conductivity k for heat conduction within the workpiece was taken as 50 W/mK, the convection and radiation boundary conditions were set in terms of Eq. (4).

$$I_{input} = \frac{2AP}{\pi \times sigx \times sigy} \times exp\left(-\left(\frac{(x-x_0)^2}{sigx^2} - \frac{(y-y_0)^2}{sigy^2}\right)\right) \quad (3)$$

I_{input} is the heat flux density of the laser beam, A is the absorptivity on the sheet metal surface, P is the laser output power, sigx and sigy are the component of laser beam along X and Y axis , and x_0, y_0 is the moving distance from the laser beam center.

$$q_{total} = q_{conv} + q_{rad} = h(T-T_0) + \varepsilon k_B(T-T_0)^4 \quad (4)$$

The heat transfer coefficient h was taken as 25W/m^{2}K, the surrounding temperature T_0 was taken as 293.15K, T is the surface temperature during the laser heating processing, ε is the emissivity chosen as 0.8 and 0.32 for heated surface with graphite coating and uncoated domains, respectively. k_B is the Stefan Boltzmann constant 5.6703x10-8 (W/m^{2}K^4).

In order to achieve more accurate simulated results as well as to ensure convergence of the solution at reasonable computing times, a dense mesh with 438 edge elements and a coarse mesh consists of 1264 domain elements were selected for the laser scanning path and remaining parts respectively. The scanning paths (Bézier Polygon) were selected from the strain fields as seen in Fig. 3.

Table 1. Process parameters chosen for overall the experiments.

Parameter	Value
Power	500W
Beam diameter	5mm
Scanning Velocity V_1	30mm/s
Laser Power Density	3.3J/mm^2
Workpiece Size	100×100×1.5mm

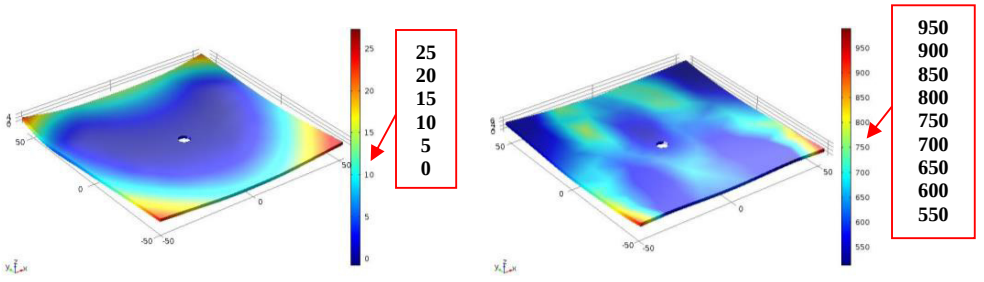

(a) (b)

Fig. 5. (a) Simulation result for deformation (mm); (b) Simulation result for temperature distribution (K)

The simulation results are presented in Fig.5 after 7 passes using strategy 3. Fig.5(a) plots the deformation results. It can be seen that the solid displacement is in the range of 0 to 25mm, of which the trend is to the target shape based on the above predefined heating parameters. The temperature field is plotted in Fig.5(b), it can be seen that the highest temperature is 950K does not exceed the S275 steel melting point (1500K to 1600K), and therefore there should be no melting on the heated surface.

3. Experimental validation

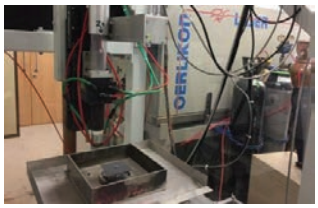

Fig. 6. Laser forming system

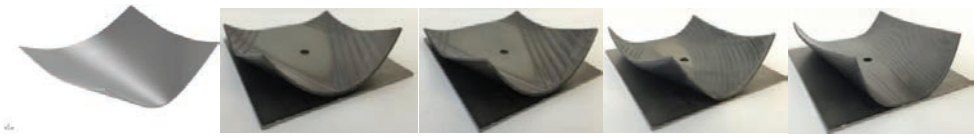

Fig. 7. Experimental formed ship hull shape by four different strategies respectively

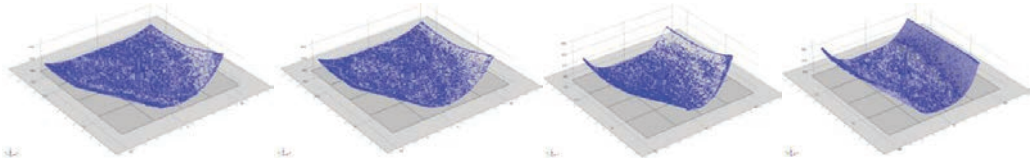

Fig. 8. The 3D laser displacement sensor scanned profiles of experimental shapes by four different strategies

The general experimental set up for the present study was shown in Fig.6. The laser system used is a PRC CO_2 laser with a maximum output power of 1.5kW. Workpiece movement is controlled by Aerotech A3200 motion control system. The workpiece was clamped through the center hole (6mm diameter) on the 3 axis CNC stage. The sequence of the scanning paths was from out to inner in order to possibly ensure the heating area of the laser spot was unchanged. The target and final formed samples are shown in Fig.7. It can be seen that the overall profile of formed shape by strategy 3 with the symmetrical dense curved paths was more similar to the target shape.

In this study, a 3D micro-epsilon scanCONTROL 2700 laser displacement sensor was used to measure the surface of the formed sample after each pass to take account of any errors due to unwanted distortion. The errors between the experimental results and target shape can be analysed based on the 3D sensor feedback data, The sensor scanned profiles are plotted in Fig.8.

4. Errors analysis

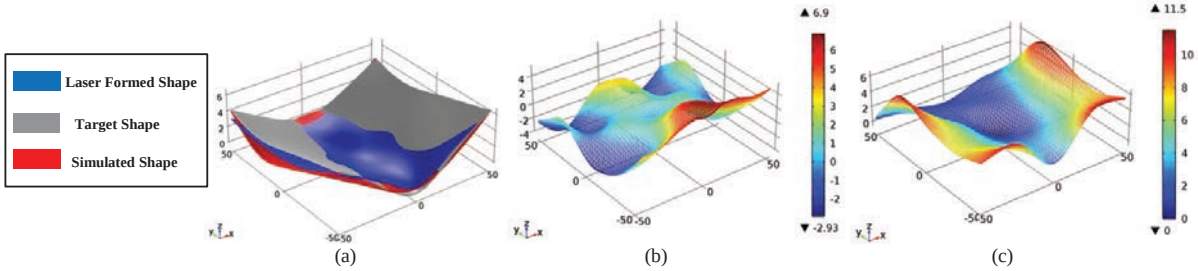

Fig. 9. (a) Laser Formed Shape, Target Shape, Simulated Shape, (b) errors between the experimental results and target shape, (c) errors between the experimental and simulated results

From Fig. 9(a), it can be seen that errors exist between the experimental and target shape in the range of 1mm to 6.9mm. Generally speaking, the errors are caused by the process planning. Therefore, the laser forming planning such as, laser scanning patterns, processing parameters and number of passes, need to be updated promptly for improving the accuracy of the formed product in a closed loop. Fig. 9(b) presents the errors between the experimental and simulated results. There are a number of factors that can lead to the errors between the simulated results and experimental results. The basic assumptions of the proposed model can be summarized as: Ideal Gaussian beam mode TEM_{00} was used in simulation while the real laser beam used in the experiment was TEM_{01}*, which could cause a different heat distribution; the initial residual stress of the workpiece was neglected in the simulation but there is likely residual stress distributed on the plate used due to manufacturing; in simulation the power input was stable, however the power during the experiment had some fluctuation around $\pm$20W errors noted.

5. Conclusions

In this paper, an investigation for the laser bending of a thin square flat sheet to a representative ship hull shape has been conducted. The overall study was conducted with FEM based 3D computational simulation and experiment verification. The strain field required to form a desired shape was obtained by a virtual press tool the initial shape to the desired shape via large-deformation elastic FEM. The symmetrical dense curved paths with the space of 3mm were preliminary determined from the synthesized strain distribution on the top surface. The predefined processing parameters including laser power, scanning velocity and beam size were determined by a range of simulation and validated by experiments. A 3D laser displacement sensor was used in the processing to measure the state of the workpieces to observe and analyse the errors during the processing. Thus, the process planning can be developed according to analysis of the errors between the experimental results and target shape.

Future research will include an investigation of advanced approaches to determine the optimal laser forming parameters corresponding to the desired deformed shape. In the simulation, the more patches will be divided on the initial shape in order to model and analyse the errors more accurately and the TEM_{01}* donut beam mode will be modelled in the simulation. It also needs to optimise the mesh size and distribution for achieving the more accurate simulated results. Moreover, the laser scanning patterns and processing parameters need to be updated promptly based on the close-loop system feedback data after each pass.

References

[1] E. Abed, S.P. Edwardson, G. Dearden and K.G. Watkins, "'GEOMETRICAL BASED CONTROL METHOD FOR 3D LASER FORMING," *Laser Assisted Net Shape Engineering 5 Proceeding of the LANE*, 2007, pp. 1043-1052.
[2] J. Cheng and L.Y. Yao, "'Process Design of Laser Forming for Three-Dimensional Thin Plates," *Journal of Manufacturing Science and Engineering*, no. 126, pp. 217-225.
[3] S.P. Edwardson, J. Griffiths, G. Dearden and K.G. Watkins, "'Towards Controlled Three-Dimensional Laser Forming,", pp. 393-399.
[4] A. James, "'Closed-loop control of product properties in metal forming: A reviewand prospectus," *Journal of Materials Processing*
[5] Kuntal Maji, "'Laser forming of a dome shaped surface: Experimental investigations, statistical analysis and neural network modeling," *Optics and Lasers in Engineering*, no. 53, pp. 31-42.
[6] A. Kyrsanidi, "'Numerical and experimental investigation of the laser forming process," *Journal of Materials Processing Technology*, no. 87, pp. 281-290.
[7] G. Labeas, "'Development of a local three-dimensional numerical simulation model for the laser forming process of aluminium components," *Journal of Materials Processing Technology*, no. 207, pp. 248-257.
[8] W. Li and L. Yao, "'Laser Forming with Constant Line Energy," *Int J Adv Manuf Technol*, no. 17, pp. 196-203.
[9] Mehdi Safari, "'Experimental investigation of laser forming of a saddle shape with spiral irradiating scheme," *Optics & Laser Technology*, no. 66, pp. 146-150.
[10] C. Peng, J. Andrew and L.Y. Yao, "'Laser Forming of Complex Structures,", April 13-14.
[11] Thomas Hennige, "'Development of irradiation strategies for 3D-laser forming," *Journal of Materials Processing Technology*, no. 103, pp. 102-108.
[12] K. Venkadeshwaran, "'Finite element simulation of 3-D laser forming by discrete section circle line heating," *International Journal of Engineering, Science and Technology*, vol. 2, no. 4, pp. 163-175.
[13] K.G. Watkins, S.P. Edwardson, J. Magee, G. Dearden, French. P, R.L. Cooke, J. Sidhu and N.J. Calder, "'Laser Forming of Aerospace Alloys," *Aerospace Manufacturing Technology Conference*, September 10-14. 2001, pp. 1-7.
[14] Shitanshu Shekhar Chakraborty, "'Parametric study on bending and thickening in laser forming of a bowl shaped surface," *Optics and Lasers in Engineering*, no. 50, pp. 1548-1558.